

# The effects of intense sound exposure on phase locking in the chick (*Gallus domesticus*) cochlear nerve

Adam C. Furman, Michael Avissar and James C. Saunders

Auditory Research Laboratory, Department of Otorhinolaryngology, Head and Neck Surgery, University of Pennsylvania, 5-Ravdin-ORL, 3400 Spruce Street, Philadelphia, PA 19104, USA

**Keywords:** chick, intense sound exposure, phase locking, synchronization, vector strength

## Abstract

Little is known about changes that occur to phase locking in the auditory nerve following exposure to intense and damaging levels of sound. The present study evaluated synchronization in the discharge patterns of cochlear nerve units collected from two groups of young chicks (*Gallus domesticus*), one shortly after removal from an exposure to a 120-dB, 900-Hz pure tone for 48 h and the other from a group of non-exposed control animals. Spontaneous activity, the characteristic frequency (CF), CF threshold and a phase-locked peri-stimulus time histogram were obtained for every unit in each group. Vector strength and temporal dispersion were calculated from these peri-stimulus time histograms, and plotted against the unit's CF. All parameters of unit responses were then compared between control and exposed units. The results in exposed units revealed that CF thresholds were elevated by 30–35 dB whereas spontaneous activity declined by 24%. In both control and exposed units a high degree of synchronization was observed in the low frequencies. The level of synchronization above approximately 0.5 kHz then systematically declined. The vector strengths in units recorded shortly after removal from the exposure were identical to those seen in control chicks. The deterioration in discharge activity of exposed units, seen in CF threshold and spontaneous activity, contrasted with the total absence of any overstimulation effect on synchronization. This suggested that synchronization arises from mechanisms unscathed by the acoustic trauma induced by the exposure.

## Introduction

Exposure to intense and damaging levels of sound in the chicken causes considerable disruption to structure and function in the peripheral auditory system. The greatest structural damage occurs to the basilar papilla within the confines of the so called 'patch' lesion (Cotanche, 1987a,b, 1999). The tectorial membrane in this lesion deteriorates entirely and is accompanied by substantial abneural hair cell loss. These hair cell losses are complemented by dramatic changes in the surface areas of supporting cells and surviving hair cells (Cotanche *et al.*, 1987; Marsh *et al.*, 1990; Saunders *et al.*, 1992). Marginal cells of the tegmentum vasculosum are also injured by the exposure (Askew *et al.*, 2006). In addition, various types of damage have been reported to the hair cell sensory hair bundle, including about a 48% loss in tip-links (Erulkar *et al.*, 1996; Husbands *et al.*, 1999; Kurian *et al.*, 2003)

Profound post-exposure changes have been reported in the activity of cochlear nerve (auditory nerve) units (Chen *et al.*, 1996; Saunders *et al.*, 1996b). Shortly after removal from the exposure, discharge activity reveals, among other things, a loss in threshold sensitivity, deterioration in frequency selectivity, a lessening of spontaneous activity and a narrowing of the dynamic range of rate-level functions (Saunders *et al.*, 1996b; Plontke *et al.*, 1999). There is also a 63% reduction in the endocochlear potential, and changes in stereocilia physiology have also been reported following both *in vivo* and

*in vitro* overstimulation (Duncan & Saunders, 2000; Szymko *et al.*, 1995).

Phase locking, a property of sound-driven discharge activity, can be identified by responses synchronized in time to a particular phase angle of a sinusoidal stimulus. This phenomenon contributes to several aspects of hearing including binaural localization and is thought to play a role in speech recognition (Geisler, 1998). Indeed, binaural hearing relies on small differences in the time of arrival at brainstem auditory nuclei, arising from discharge activity originating in the auditory nerve from each ear (Goldberg & Brown, 1969; Carr & Konishi, 1988). In addition, the periodic representation of the stimulus plays an important role in the neural representation of pitch, either through phase locking in individual neurons or through periodic discharges in ensembles of neurons (i.e. neural volleying, Wever, 1949).

Time resolution or synchrony in auditory neurons of various songbirds was first reported by Konishi (1969). His results suggested that birds were 'clearly superior to typical mammals in time resolution.' In more recent work with avian species such as the red-winged black bird, starling or pigeon, phase locking is maintained at frequencies as high as 4.0 kHz (Sachs *et al.*, 1980; Gleich & Narins, 1988; Hill *et al.*, 1989; Manley *et al.*, 1997). Remarkably, the barn owl exhibits phase locking to 10.0 kHz (Köppel, 1997). Phase locking has also been reported for the adult chicken and synchronization to approximately 2.0 kHz was noted (Salvi *et al.*, 1992).

The effects of sound exposure on phase locking in the discharge patterns of cochlear nerve units of the chick, or any avian species, remain to be described in detail. Given the profound structural and

Correspondence: Adam Furman, as above.

E-mail: acfurman@mail.med.upenn.edu

Received 10 May 2006, revised 22 June 2006, accepted 25 July 2006

functional changes in the auditory periphery noted above, we would anticipate degradation of cochlear nerve phase locking in the overstimulated animal. The current study was designed to examine this prediction.

## Materials and methods

### *Animal groups and sound exposure*

White leghorn chicks (*Gallus domesticus*) between 5 and 15 days of age were formed into non-exposed and exposed groups. The control group was kept in brooders until testing. The exposed group was overstimulated with a 120-dB SPL pure tone at 0.9 kHz for 48 h. This exposure frequency was chosen so that the current results would be compatible with many other studies utilizing the same exposure condition (see e.g. Saunders & Salvi, 2006). Moreover, the 0.9-kHz frequency lies in the region of best hearing for the chick. The exposure took place in a sound-attenuated chamber with chicks individually housed in a segmented, circular, wire-mesh cage suspended beneath a 30-cm low-frequency speaker. The sound was measured with a 6.25-mm condenser microphone and expressed as dB re 20  $\mu$ Pa. The variability in exposure intensity averaged  $\pm 1.0$  dB in each segment of the cage. Details of the exposure can be found elsewhere (Saunders *et al.*, 1996b; Lifshitz *et al.*, 2004). The treatment and care of chicks in this study followed procedures approved by the Institutional Animal Care and Use Committee of the University of Pennsylvania.

### *Animal preparation*

Chicks were anesthetized immediately after removal from the exposure with an intramuscular injection of 25% ethyl carbamate solution (Urethane). The dosage was 0.1 ml/10 g of body weight and anesthesia was gauged by the absence of a toe-pinch reflex. Free breathing was assured through a tracheotomy. The skull was exposed and affixed to a head holder with a cyano-acrylate glue and poly methylmethacrylate cement (CrazyGlue<sup>®</sup> and dental cement). The left tympanic membrane was exposed by removing the tissue forming the ear canal and a small hole approximately 3–4 mm in diameter was opened in the outer layer of the temporal bone medial and posterior to the ear canal. This opening allowed access to the inner bony layer of the skull over the capsule of the cochlea. The inner bony layer was carefully removed taking care to leave the membranous layer of the cochlear capsule intact. Once all bone fragments were cleared from this hole, the capsule was gently pierced with a microdissection pick, exposing the recessus scala tympani. On the medial wall of the scala tympani, the cochlear ganglion could be visualized as a horizontal white band, which was the target for the recording electrode.

### *Cochlear nerve recordings*

Recording electrodes were made from borosilicate capillary glass tubing (M120F4, WPI Inc., Sarasota, FL, USA), filled with 3 M KCl, with final resistances between 15 and 30 M $\Omega$ . The electrode was mounted on a microdriver and advanced through the peri-lymph in 1- $\mu$ m steps until it entered the cochlear ganglia. Amplified nerve discharges detected by the electrode were converted to square wave pulses with a level detector and the time between discharges was determined with an event timer. A computer organized and stored the timing of nerve discharges.

Sound stimuli were generated with a frequency synthesizer (Audio Precision System One, Beaverton, OR, USA) with amplitude and

frequency under computer control. Acoustic signals were produced with an earphone (model DT48, Beyer Dynamic, Hicksville, NY, USA) whose output was coupled to the tympanic membrane through a sound tube. The sound tube was sealed over the tympanic membrane. Acoustic stimuli were calibrated with a 0.5-mm probe-tube microphone (model ER-7, Entymotic Research, Elk Grove Village, IL, USA) inserted in the center of the sound tube and located approximately 2 mm in front of the tympanic membrane. The analyser section of System One detected the microphone response and converted it to dB SPL (re 20  $\mu$ Pa).

A wide-band noise between 80 and 90 dB SPL was presented in 40-ms sound bursts (2.5-ms rise and fall time) and used as a search stimulus to identify units responding to auditory stimuli. When a cochlear nerve unit was identified, it was characterized by measuring the rate of spontaneous activity and a tuning curve. The tuning curve was used to determine the characteristic frequency (CF). In addition, a rate-intensity function was obtained at the CF for stimuli between 10 and 100 dB SPL in 3.3-dB steps. From the rate-intensity function, the CF threshold could be accurately determined as that point where the curve shifted from spontaneous activity to sound-driven activity. The procedures for measuring these characteristics have been detailed elsewhere (Lifshitz *et al.*, 2004; Saunders *et al.*, 1996b, 2002).

### *Peri-stimulus time histogram*

A 40.0-ms pure-tone burst with a rise and decay time of 2.5 ms, at the unit's CF, was presented repeatedly 20 dB above the CF threshold. These stimuli were synchronized such that each burst began at the same phase angle. Each time the tone burst was presented, the discharge pattern from the cochlear nerve unit was recorded and added to a peri-stimulus time histogram (PSTH). The discharges were obtained with a temporal resolution of 10  $\mu$ s, and between 300 and 400 tone bursts were presented in constructing the PSTH. A 400-ms interval existed between tones bursts, which was much longer than the time constant for recovery from adaptation (Spassova *et al.*, 2004). These histograms were used in all subsequent analysis.

There are two possible strategies for selecting an appropriate stimulus intensity that allows a fair comparison of control and exposed units. The first selects a criterion dB level above the CF threshold and then measures all PSTHs at that condition. The second selects a criterion discharge rate and adjusts the stimulus level accordingly. This second strategy may resolve differences between rate-level functions in control and exposed units (Saunders *et al.*, 1996b; Plontke *et al.*, 1999). In this presentation, we chose to use the first method because discharge rates among units varied greatly across all units, meaning that a criterion response level achievable in one unit may not be possible in another.

### *Period histograms*

Using the PSTH data for each unit, a period histogram was generated. The period histogram displayed the number of neural discharges at every phase of the repeated acoustic stimulus, where phase ranged from 0 to  $2\pi$ . This effectively replotted the PSTH into a representation of discharge activity in the phase domain.

### *Vector strength*

The method used here for measuring the degree of synchronization, or phase locking, determines the vector strength (*V/S*) from the responses contained in the PSTHs, as originally described by Goldberg & Brown

(1969).  $VS$  is a unit-less measure that describes the synchrony of a unit discharge relative to a periodic stimulus and is defined by

$$VS = \frac{\sqrt{(\sum \cos \theta_i)^2 + (\sum \sin \theta_i)^2}}{n} \quad (1)$$

where  $\theta_i$  is the corresponding phase angle for each neural discharge and  $n$  represents the total number of discharges.  $VS$  was calculated by iterating the above summations with all responses from the same unit. This calculation was then repeated for all units and the magnitude of  $VS$  was plotted against unit CF. A  $VS$  of 1 denotes perfect synchrony whereas a  $VS$  of 0 is a random, unsynchronized phase distribution.

#### Temporal dispersion

Temporal dispersion measures the absolute variability in spike timing. This parameter constitutes a conversion from the unit-less  $VS$  calculation to an indication of variability described in the time domain and is expressed in seconds. The dispersion is the SD of a Gaussian distribution that has the same  $VS$  measured from the unit's response. Temporal dispersion is defined by

$$\text{Temporal dispersion} = \frac{\sqrt{-2 \ln VS}}{2\pi f} \quad (2)$$

where  $f$  is the stimulus frequency and  $VS$  is the vector strength calculated from Eqn 1. By assuming a Gaussian distribution as suggested by Paolini *et al.* (2001) instead of a rectangular distribution as used in previous studies (Hill *et al.*, 1989), the calculation remains more accurate at low  $VS$  values. Paolini *et al.* (2001) covered the mathematical derivation of this formula in detail. The magnitude of temporal dispersion was plotted against the CF of each unit.

#### Statistical analysis

The Rayleigh likelihood test determines the statistical reliability of periodicity. It was utilized here to determine if the measure of  $VS$  was statistically significant, meaning that the periodic component occurred at a greater than chance level. Rayleigh likelihood, based on the Rayleigh distribution (Mardia, 1972; Papoulis, 1984; Narins & Wagner, 1989), was calculated by

$$L = 2n(VS)^2 \quad (3)$$

where  $L$  is the Rayleigh likelihood number,  $VS$  is the vector strength from Eqn 1 and  $n$  is the number of discharges. An  $L$ -value of 13.8 corresponds to a probability level of 0.001, which was used as the criterion for significant phase locking.

## Results

### Effects of overstimulation on characteristic frequency threshold and spontaneous activity

Data were collected from 240 and 170 well-isolated control and exposed units, respectively. Tuning curves, rate-level functions and spontaneous activity were obtained for each of these units. Control unit CF thresholds appear in Fig. 1 and approximated those reported previously for chicks (Saunders *et al.*, 1996b). The control units had higher CF thresholds at the lowest and highest frequencies with the most sensitive thresholds (lowest) observed between 0.6 and

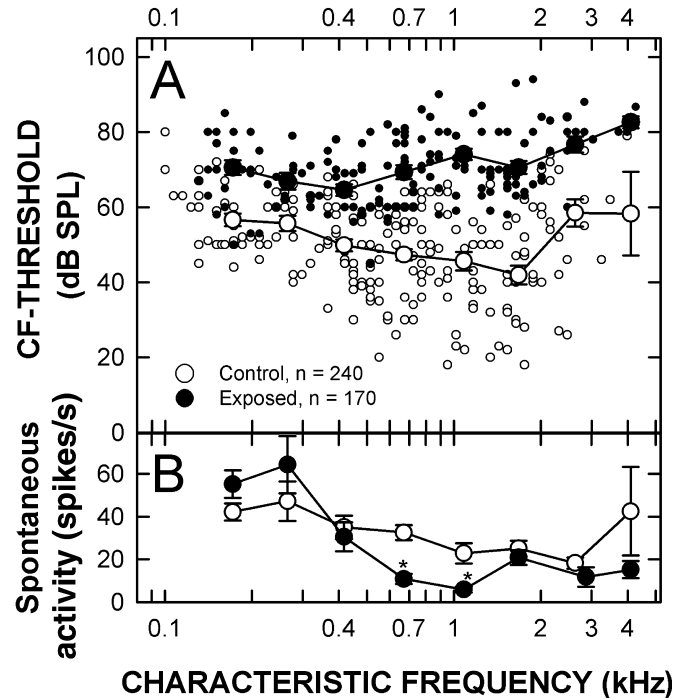


FIG. 1. (A) The characteristic frequency (CF) thresholds are plotted for a sample of units obtained in non-exposed control chicks and chicks tested within a few hours of removal from the exposure. The large symbols indicate the average CF threshold calculated over successive frequency bins (approximately 3/4 octaves), whereas the error bars represent  $\pm 1$  SEM. The poorer thresholds of exposed units are apparent. (B) Mean values for spontaneous activity are plotted against CF. \*Statistically significant difference between exposed and control chicks at that frequency.

1.5 kHz. The exposed CF thresholds in Fig. 1A were generally higher than seen in controls and were similar to previous reports of unit thresholds obtained in exposed chicks shortly after removal from the exposure (Saunders *et al.*, 1996b). The range of unit CFs was organized into eight equally spaced intervals (on the logarithmic scale, approximately 3/4-octave bins) and the CF thresholds for units contained within each interval were averaged separately for control and exposed data. In each bin, CF thresholds in the exposed group were higher than in the control; however, the difference between groups was frequency dependent. The amount of threshold shift in the exposed units was least in the lowest and highest frequency bins at approximately 20 dB, whereas between 0.7 and 2.0 kHz it was 30–35 dB.

A two-way ANOVA, with factors of group and frequency, revealed a significant frequency effect. More importantly, there was a significant difference between the control and exposed group, and a paired comparison evaluation indicated reliable group differences for each frequency bin ( $P < 0.05$ ). The interaction term between the frequency and group factor was not significant.

The spontaneous rate in the exposed units was also depressed as seen in Fig. 1B. Spontaneous discharges for control cells in bins between 0.5 and 1.2 kHz averaged approximately  $28 \pm 4.1$  spikes/s ( $\pm$  SEM), whereas in the exposed group it was approximately  $8 \pm 1.82$  spikes/s. The 20 spike/s reduction in the exposed group activity was statistically significant ( $P < 0.05$ ) and was similar to that previously reported in young and adult chickens (Chen *et al.*, 1996; Saunders *et al.*, 1996b). There was no difference in spontaneous activity between control and exposed units in bins below 0.5 kHz or above 1.2 kHz.

Although the data are not reported here, tuning curve selectivity deteriorated and the slope of rate-intensity functions increased as previously reported (Pugliano *et al.*, 1993; Saunders *et al.*, 1996b). Thus, the exposure had a substantial deleterious effect on cochlear nerve activity and supported the expected observation that acoustic trauma to the chick inner ear profoundly alters peripheral auditory function.

### Synchronization in peri-stimulus time histograms

Figure 2 presents PSTHs from representative low-, mid- and high-CF control units responding to a 40-ms phase-locked tone burst. The degree of synchronization in the low-frequency unit in the top panel is obvious and the interval between peaks corresponds to the 0.2-kHz stimulus. There was a delay in the system due to acoustic and physiological conduction time, with the actual acoustic signal activating the cochlear nerve fiber within several milliseconds of the onset of the histogram recording. Interestingly, activity between peaks of sound-driven activity in the low-frequency unit is largely suppressed during the stimulus presentation. The 1.0-kHz mid-frequency example in the middle panel reveals a less pronounced degree of synchronization in that the variance from one peak of synchronized activity to the next is beginning to blur the distinction between adjacent peaks. The 3.2-kHz PSTH example in the bottom panel of Fig. 2 exhibits clear evidence of periodic discharge activity; however, periodicity is less pronounced. Visually, the decrease in

depth between adjacent peaks and troughs represents a degradation of temporal structure as the unit response becomes less synchronized to the stimulus.

### Synchronization in period histograms

The ability to phase lock may be visualized in the period histogram. This analysis of period histograms permits insight into phase angle variability within each stimulus cycle. The phase angle of every neural discharge from one unit was calculated. The discharge angles were organized as a histogram with the ordinate axis ranging from 0 to  $2\pi$ . The resulting plot showed the phase angle distribution for all discharges in that unit. Figure 3 plots period histograms for the three units presented in Fig. 2. The graphs in Fig. 3A were centred at  $\pi$  to allow for easy comparison between units.

The low-frequency (0.2-kHz) unit in Fig. 3A exhibits a sharp peak with a *VS* of 0.92. However, as CF increases, the period histogram broadens, and phase specificity declines which is revealed in the lower *VS*s of 0.59 and 0.24 for the units with CFs of 1.0 and 3.2 kHz. However, the amount of time represented by each periodic response becomes shorter with increasing frequency (Fig. 3B) and therefore so does the variability in time, as seen in the decreasing values of temporal dispersion (0.38, 0.14 and 0.06 ms).

### Synchronization in control and exposed units

The 10- $\mu$ s resolution of the PSTH allowed for accurate calculation of *VS* and, when plotted against CF in Fig. 4, revealed that synchronization remained high and relatively constant at low frequencies. Above approximately 0.5 kHz *VS* steadily declines and is minimal in the highest CF units. *VS*, temporal dispersion and the Rayleigh number were calculated for all 410 units reported in this study and in 407 of these the Rayleigh statistic exhibited an *L*-value  $\geq 13.8$ , which indicated that phase locking had a significant probability of non-uniformity ( $P < 0.001$ ). The Rayleigh likelihood test revealed that statistically significant phase locking occurred in both control and exposed animals at all CFs. Only three exposed units, at approximately 3.8 kHz, did not pass the Rayleigh likelihood test, although units with higher CF continued to synchronize. These three units are marked with a star in Fig. 4. We were unable to record units with CFs higher than 4.2 kHz because of limitations in accessing the cochlear nerve through the scala tympani (Manley *et al.*, 1991; Salvi *et al.*, 1994). The identification of reliable synchronization in chick units as high as 4.2 kHz is consistent with the observation of synchronized cochlear nerve activity in other avian species (see examples in Köppl, 1997).

Figure 4 also distinguishes *VS*s for control and exposed units. The large symbols indicate the mean *VS* level for the respective group when the data were binned in progressive logarithmic intervals. A two-way ANOVA was undertaken on the binned data with one factor being group and the second being frequency. As might be expected, *VS* changed with frequency in a significant manner ( $P < 0.001$ ). The group factor, however, showed no difference between control and exposed units ( $P > 0.05$ ). Similarly, there was no difference in the interaction term between group and frequency.

### Temporal dispersion

Temporal dispersion, an indication of the variability of synchronization in the time domain, is plotted as a function of unit CF in Fig. 5. The data were binned in the same way as previously described and

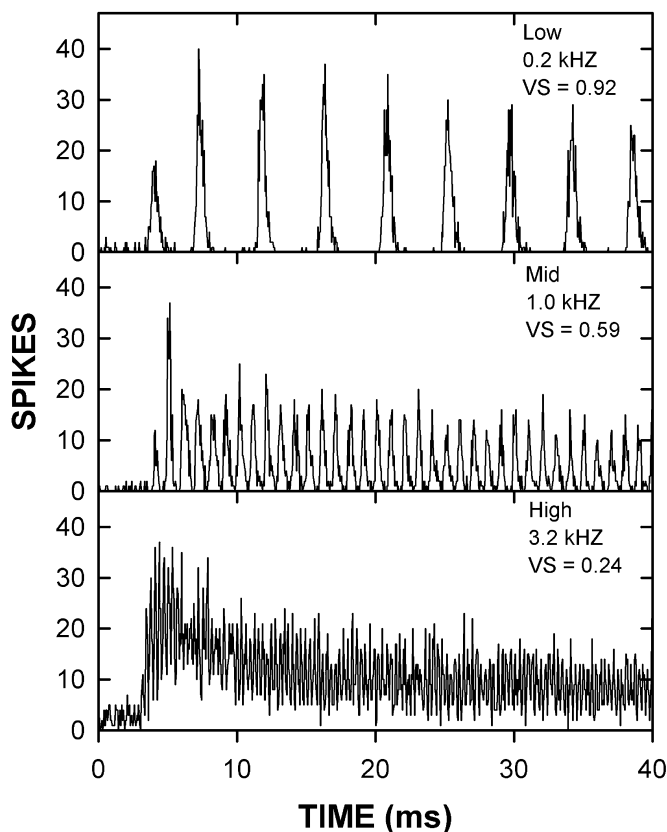


FIG. 2. The peri-stimulus time histogram of three representative control units is shown in the three panels for a low, mid and high characteristic frequency unit, respectively. Periodicity is clearly visible in each example, although it becomes less apparent into the high frequencies.

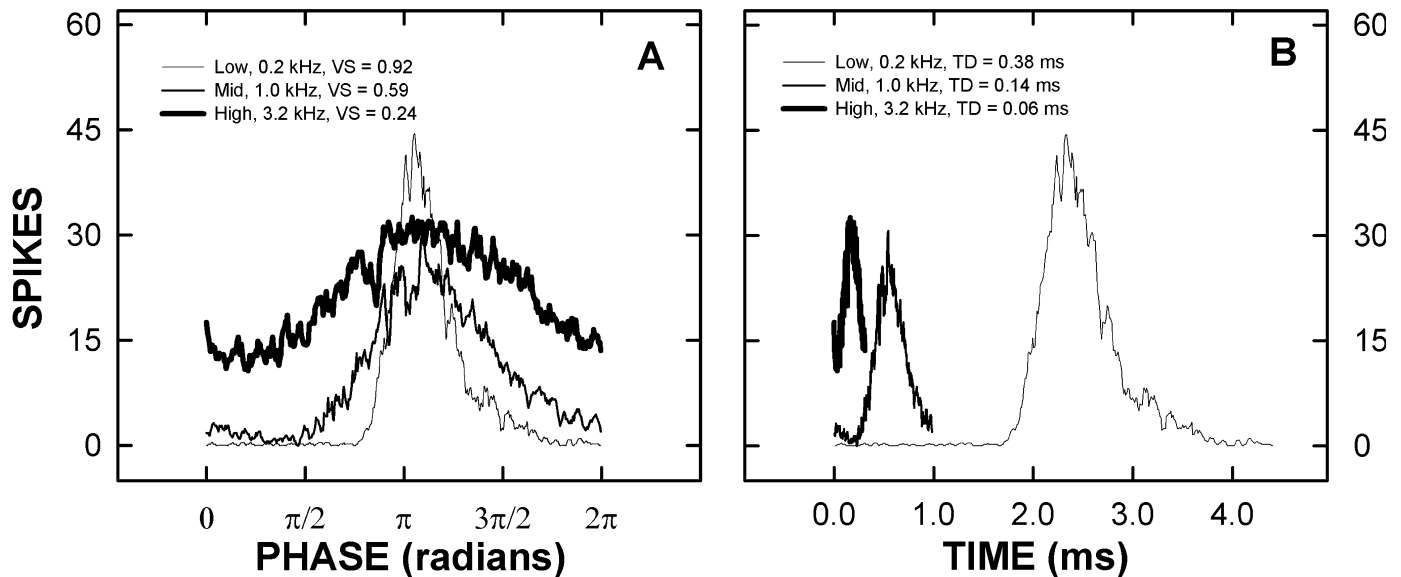


FIG. 3. Examples of a period histogram are shown for the same three units presented in Fig. 2. (A) Histograms are plotted against phase angle to illustrate the decrease in phase specificity as the characteristic frequency increases. (B) Histograms are plotted against time in order to emphasize the increasing temporal precision as the characteristic frequency increases.

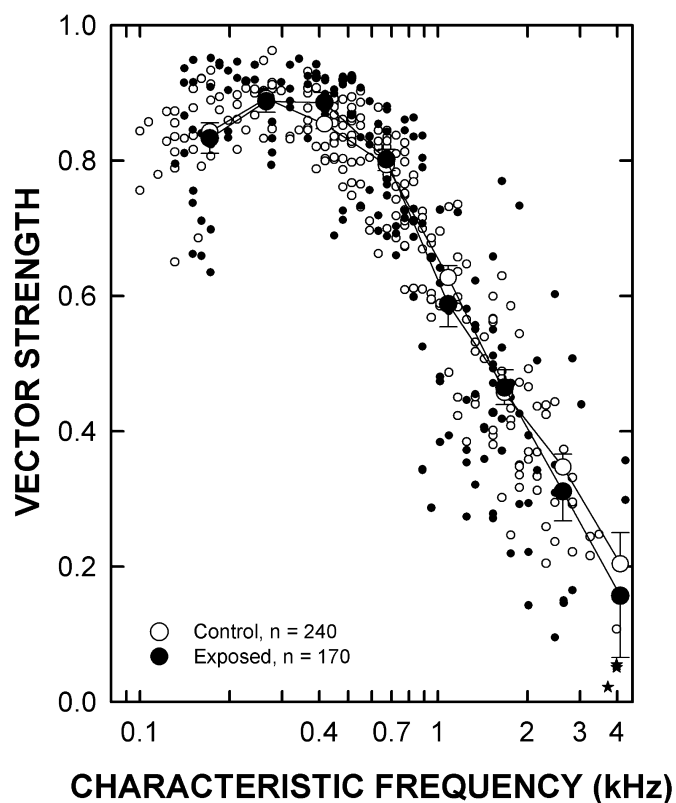


FIG. 4. Vector strength is plotted against unit characteristic frequency for control and exposed units. The large symbols and solid lines indicate the results for data binned in successive frequency intervals, whereas the error bars show  $\pm 1$  SEM about the mean. Statistical analysis (see text) revealed that the results from the control and exposed groups came from overlapping populations. \*Three exposed units that did not meet the Rayleigh criteria.

then compared between control and exposed conditions. Figure 5 reveals that the variability (dispersion) of synchronization, in the time domain, is greatest in the low frequencies but lessens

systematically as CF increases, reaching the least degree of variability at the highest CFs examined. Thus, variability in the synchronized response, as CF increases, becomes more precise in the time domain even though it deteriorated in the phase domain (Fig. 4). As would be predicted from the results in Fig. 5, the differences between groups in temporal dispersion were due to random sampling (ANOVA,  $P > 0.05$ ). At any recorded frequency, values of dispersion were similar to those reported in the owl and rat (Köppl, 1997; Paolini *et al.*, 2001).

The period histograms in Fig. 3 unify the observation of decreasing *VS* and decreasing temporal dispersion as frequency increases. As the results in Figs 4 and 5 show, these changes were consistent and orderly across CF. Moreover, the changes in the per-stimulus time or period histograms, with increasing CF, were the same for both examples in Fig. 3. This observation contrasts with the results in Fig. 1, where the exposure had a profound effect on CF threshold.

#### Mean phase response

In addition to the degree of synchronization, over-stimulation could affect the response latency of the cochlear nerve. This could manifest itself as a change in the mean response phase in single units after sound exposure. The absolute mean phase response for each unit was not known due to variable physiological conduction times. However, a systematic change in the response latency should still be observable in the population of cells as a relative change in mean response phase between control and exposed units. Figure 6 plots the mean phase for each frequency bin, normalized so that the control units at each bin are set to zero, and then adjusts the exposed phase accordingly. As can be seen, the difference between groups was due to random sampling (ANOVA,  $P > 0.05$ ). This suggests that, in addition to synchronization, the latency of the system was similarly unaffected. Although unlikely, there is no way to eliminate the possibility that the sound exposure caused a full cycle shift in phase, which would not be detected with the methods presently used.

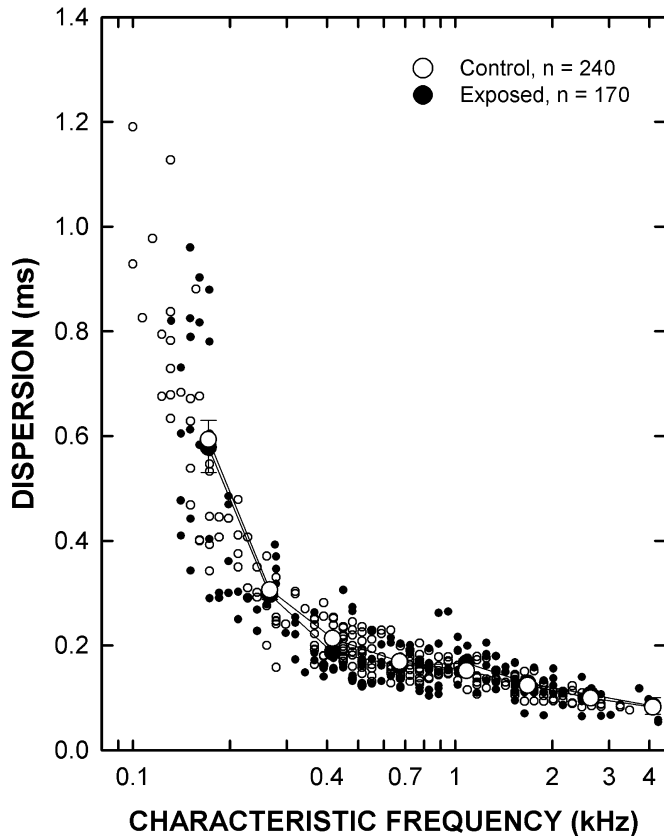


FIG. 5. Temporal dispersion is plotted for each unit by characteristic frequency (CF) and distinguished by the control or exposed group. The variability in the phase-locked response becomes systematically shorter as the unit CF increases. The large symbols describe the dispersion across the successive bins and the bars indicate  $\pm 1$  SEM. No differences were observed between control and exposed units.

## Discussion

### *Effects of intense sound exposure*

The most important observation in this presentation was the similarity in *V*Ss between the exposed and control groups. This observation failed to support the anticipation in the Introduction that there would be a substantial difference between groups. Moreover, the absence of any difference in synchronization occurred despite the deleterious effect that intense sound had on other aspects of the cochlear nerve response.

The structural consequences of a 120-dB exposure in chicks are well documented in other studies employing the same conditions (Saunders *et al.*, 1992, 1996a,b; Cotanche, 1999). This exposure caused massive trauma to the inner ear focused primarily in a discrete region on the abneural side of the basilar papilla at the corresponding tonotopic location of the 0.9-kHz tone (Cotanche, 1987a). The injury sustained in this area consisted of hair cell loss, reorganization of the basilar papilla surface, destruction of the tectorial membrane, damage to the dark cells of the tegmentum vasculosum and tip-link loss on surviving hair bundles. The acoustic damage in the chick inner ear following a 120-dB 48-h pure tone exposure is the same across many publications (see review by Cotanche, 1999) and there is every reason to believe that the chicks in the present study exhibited similar structural damage.

Injury to the chick tegmentum or increased ion permeability in the walls of scala media could account for the previously reported 63%

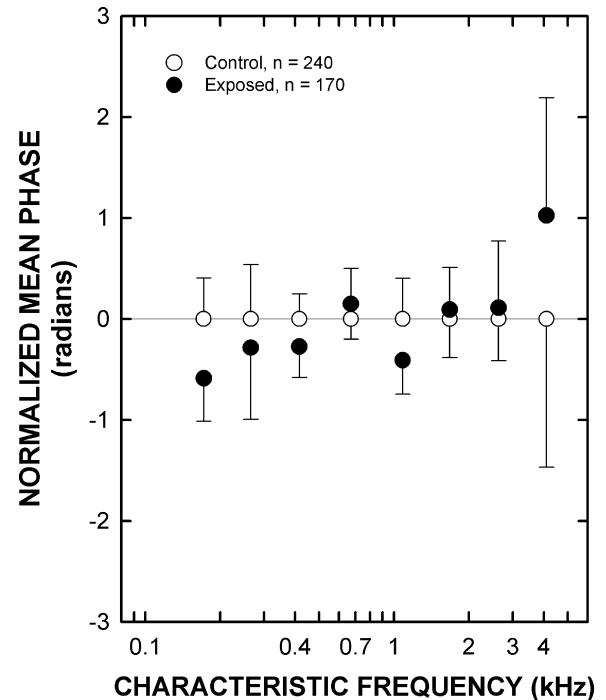


FIG. 6. The mean phase angle is plotted for the control and exposed units after normalizing the data by setting each control bin equal to zero. No differences were observed between the two groups.

reduction in the endocochlear potential (Poje *et al.*, 1995; Rama-krishna *et al.*, 2004). Tip-link damage would be expected to compromise the input to the hair cell, reducing membrane receptor currents during hair bundle stimulation (Husbands *et al.*, 1999; Kurian *et al.*, 2003). The depolymerized tectorial membrane in the patch might contribute to a reduction in the way basilar membrane movements are translated into sensory hair bundle displacement on neural hair cells (McFadden & Saunders, 1989; Smolders *et al.*, 1995; Saunders *et al.*, 1996b). These changes could all contribute to the loss in threshold sensitivity at CF. A specific cause-and-effect relationship between these injuries and changes in cochlear nerve activity has yet to be demonstrated; however, their net effect is evident after overstimulation in the changed CF thresholds of Fig. 1 and the reduction in spontaneous activity.

The challenge posed by the results in this study is to explain how the acoustic injuries contribute to deterioration in CF threshold and spontaneous activity but leave synchronization unaffected. One interpretation of the results is that acoustic trauma damaged those processes that contribute to hair cell input but had no effect on the membrane properties or the intracellular hair cell machinery associated with the synchronized release of neurotransmitter. To understand this dichotomy it is useful to appreciate the hair cell events that lead to cochlear nerve synchronization.

### *Mechanisms that determine cochlear nerve synchronization*

Phase locking at the cochlear nerve is the end result of a cascade of events in the peripheral ear that are all synchronized to the stimulus. Sinusoidal movements of the stereocilia gate transduction channels in a precisely defined cyclical manner. Consequently, the probability of any given transduction channel being open depends upon the magnitude and direction of hair bundle deflection (Assad *et al.*,

1991). The correlation between hair cell receptor potential and neural discharges has been well defined in the guinea-pig (Palmer & Russell, 1986). At low frequencies the membrane depolarizes in synchrony with the excitatory hair bundle deflections and this is represented in the synchronized neural discharges in Fig. 2. However, the membrane depolarization occurs only during the excitatory half cycle of hair bundle displacement, thus functioning like a half-wave rectifier. The membrane time constant creates a low-pass filter and, as frequency increases, this smoothes the half-rectified membrane potential to a steadier potential, with a decreasing overlaid ripple (Palmer & Russell, 1986).

The depolarizing phase of the receptor potential activates voltage-dependent L-type calcium channels (Hudspeth & Lewis, 1988; Fuchs *et al.*, 1990; Zidanic & Fuchs, 1995) and triggers the exocytosis of synaptic vesicles (Brandt *et al.*, 2003; Parsons *et al.*, 1994; Moser & Beutner, 2000; Spassova *et al.*, 2001). The secreted glutamate traverses the synaptic cleft to bind with AMPA receptors on the post-synaptic membrane (Glowatzki & Fuchs, 2002), which in turn trigger post-synaptic events leading to a neuronal discharge (Siegel, 1992). At low frequencies the post-synaptic discharges are perfectly synchronous with hair bundle movements on a cycle-per-cycle basis, and this is evident in the high level of *VS* between 0.1 and 0.5 kHz (Fig. 4). By inference, the intervening steps in the excitation–secretion coupling cascade are also synchronized. As frequency increases, however, the low-pass filtering properties of the membrane produce a DC component in the receptor potential (Kidd & Weiss, 1990), which degrades the phasic entry of calcium into the hair cell. At higher frequencies the calcium diffusion and buffering properties of the intracellular environment further degrade the synchronized release of neurotransmitter, and hence blur the synchronized discharges at the neuron terminal. Finally, at a sufficiently high frequency the membrane enters a steady state of depolarization and calcium enters the hair cell nearly continuously. Thus, at high frequencies, the probability of exocytosis is more uniform throughout stimulation and neuron activation exhibits little synchronization. This array of cascading events suggests that the hair cell membrane and synaptic physiology specifically associated with the phenomena of synchronization were functionally unchanged, and largely independent of the surrounding acoustic trauma to the basilar papilla.

The question remains as to why structural trauma to the basilar papilla did not affect the synchronization mechanisms in the hair cell. The answer to this question is inconclusive but the following is a possibility. Hair bundle motion arises from shear forces established by the sliding movements between the tectorial membrane and the reticular surface due to displacements of the basilar membrane (Smolders *et al.*, 1995; Saunders *et al.*, 1996b). When the tectorial membrane in the patch lesion depolymerizes, within a few hours of exposure onset (Cotanche, 1999; Cotanche *et al.*, 1991), it would be expected to reduce or remove the mechanical input to the hair cells (McFadden & Saunders, 1989; Saunders *et al.*, 1996b). The decoupling of the mechanical input to the hair cells means that they may incur little further injury during the additional 40+ h of the exposure. Although the intracellular environment of the hair cell might be traumatized early in the exposure, it may suffer little further injury after tectorial membrane destruction and might even recover during continuing overstimulation. This is supported by 200-h exposures in which regenerated hair cells emerged in the lesion area while the exposure was still in progress (Pugliano *et al.*, 1993). The answer to the question posed above may be found in overstimulation failing to traumatize the hair cell mechanisms of synchronization because the mechanical input to the apical pole of the hair cell was decoupled from the traumatic stimulus.

### Changes in spontaneous activity

There are two likely sources for spontaneous activity, with one representing stochastic gating of the stereocilia transduction channels (from acoustic noise or Brownian motion in the surrounding fluids) and the other being stochastic vesicle exocytosis at the hair cell synapse. If the synapse was unaffected by the exposure as suggested above, then spontaneous activity with a synaptic origin should have been the same in control and exposed units. However, the sound exposure caused a significant decrease in spontaneous activity, suggesting that these responses arise from stochastic openings of the stereocilia transduction channels. The reduction in spontaneous activity may be associated with the damage to the stereocilia following exposure which would be expected to disrupt channel gating (Saunders *et al.*, 1985; Erulkar *et al.*, 1996; Husbands *et al.*, 1999; Kurian *et al.*, 2003).

There also exists evidence for an active amplifier in non-mammalian vertebrates occurring at the level of the hair bundle (Hudspeth, 1997; Manley & Köppl, 1998). This amplifier may result in spontaneous stereocilia motion and channel gating, leading to spontaneous activity seen in the auditory nerve. The random motion of the hair bundle is more than would be predicted from Brownian movements in the endolymph (Martin & Hudspeth, 1999) and should be enough to account for the spontaneous discharges seen in auditory nerves of non-exposed chicks.

### Conclusions

Synchronization has been reported in cochlear nerve units of the adult chicken (Salvi *et al.*, 1992), red-winged black bird (Sachs *et al.*, 1980), starling (Gleich & Narins, 1988), emu (Manley *et al.*, 1997) and pigeon (Hill *et al.*, 1989), and in these species it exhibits a similar pattern across frequency as reported here. The results also indicate that in spite of considerable acoustic trauma to the chick basilar papilla and significant changes in cochlear nerve unit CF threshold and spontaneous activity, the properties of synchronization were unchanged. It was proposed that this unexpected and dichotomous observation may be due to the manner in which overstimulation in the chick affects the functional capability of the inner ear. The exposure may alter the mechanisms that control the input signals to the hair cells but leave intact the intracellular machinery that controls the process of synchronization.

### Acknowledgements

The authors appreciate the comments and suggestions of Shunda Irons Brown, Michael Anne Gratton, Matthew Giampoala and Thomas D. Parsons. This research was supported by awards from the Pennsylvania Lions Hearing Research Foundation and the NIDCD (DC 000710) to J.C.S.

### Abbreviations

CF, characteristic frequency; PSTH, peri-stimulus time histogram; *VS*, vector strength.

### References

- Askew, C., Saunders, J.C. & Gratton, M.A. (2006) Ultrastructural analysis of the Tegmentum Vasculosum after intense sound. *Abstr. Assoc. Res. Otolaryngol.*, **29**, 14.
- Assad, J.A., Shepherd, G.M. & Corey, D.P. (1991) Tip-link integrity and mechanical transduction in vertebrate hair cells. *Neuron*, **7**, 985–994.
- Brandt, A., Striessnig, J. & Moser, T. (2003) CaV1.3 channels are essential for development and presynaptic activity of cochlear inner hair cells. *J. Neurosci.*, **23**, 10 832–10 840.
- Carr, C.E. & Konishi, M. (1988) Axonal delay lines for time measurement in the owl's brainstem. *Proc. Natl Acad. Sci. U.S.A.*, **85**, 8311–8315.

- Chen, L., Trautwein, P.G., Shero, M. & Salvi, R.J. (1996) Tuning, spontaneous activity and tonotopic map in chicken cochlear ganglion neurons following sound-induced hair cell loss and regeneration. *Hear. Res.*, **98**, 152–164.
- Cotanche, D.A. (1987a) Regeneration of hair cell stereociliary bundles in the chick cochlea following severe acoustic trauma. *Hear. Res.*, **30**, 181–195.
- Cotanche, D.A. (1987b) Regeneration of the tectorial membrane in the chick cochlea following severe acoustic trauma. *Hear. Res.*, **30**, 197–206.
- Cotanche, D.A. (1999) Structural recovery from sound and aminoglycoside damage in the avian cochlea. *Audiol. Neurootol.*, **4**, 271–285.
- Cotanche, D.A., Saunders, J.C. & Tilney, L.G. (1987) Hair cell damage produced by acoustic trauma in the chick cochlea. *Hear. Res.*, **25**, 267–286.
- Cotanche, D.A., Petrell, A. & Picard, D.A. (1991) Structural reorganization of hair cells and supporting cells during noise damage, recovery and regeneration in the chick cochlea. *Ciba Found. Symp.*, **160**, 131–142; discussion 142–150.
- Duncan, R.K. & Saunders, J.C. (2000) Stereocilium injury mediates hair bundle stiffness loss and recovery following intense water-jet stimulation. *J. Comp. Physiol. [A]*, **186**, 1095–1106.
- Erukhar, J.S., O'Brien, D.A. & Saunders, J.C. (1996) Hair bundle morphology on surviving hair cells of the chick basilar papilla exposed to intense sound. *Scann. Microsc.*, **10**, 1127–1140; discussion 1140–1142.
- Fuchs, P.A., Evans, M.G. & Murrow, B.W. (1990) Calcium currents in hair cells isolated from the cochlea of the chick. *J. Physiol.*, **429**, 553–568.
- Geisler, C.D. (1998) *From Sound to Synapse: Physiology of the Mammalian Ear*. Oxford University Press, New York.
- Gleich, O. & Narins, P.M. (1988) The phase response of primary auditory afferents in a songbird (*Sturnus vulgaris* L.). *Hear. Res.*, **32**, 81–91.
- Glowatzki, E. & Fuchs, P.A. (2002) Transmitter release at the hair cell ribbon synapse. *Nat. Neurosci.*, **5**, 147–154.
- Goldberg, J.M. & Brown, P.B. (1969) Response of binaural neurons of dog superior olivary complex to dichotic tonal stimuli: some physiological mechanisms of sound localization. *J. Neurophysiol.*, **32**, 613–636.
- Hill, K.G., Stange, G. & Mo, J. (1989) Temporal synchronization in the primary auditory response in the pigeon. *Hear. Res.*, **39**, 63–73.
- Hudspeth, A. (1997) Mechanical amplification of stimuli by hair cells. *Curr. Opin. Neurobiol.*, **7**, 480–486.
- Hudspeth, A.J. & Lewis, R.S. (1988) Kinetic analysis of voltage- and ion-dependent conductances in saccular hair cells of the bull-frog, *Rana catesbeiana*. *J. Physiol.*, **400**, 237–274.
- Husbands, J.M., Steinberg, S.A., Kurian, R. & Saunders, J.C. (1999) Tip-link integrity on chick tall hair cell stereocilia following intense sound exposure. *Hear. Res.*, **135**, 135–145.
- Kidd, R.C. & Weiss, T.F. (1990) Mechanisms that degrade timing information in the cochlea. *Hear. Res.*, **49**, 181–207.
- Konishi, M. (1969) Time resolution by single auditory neurones in birds. *Nature*, **222**, 566–567.
- Köpl, C. (1997) Phase locking to high frequencies in the auditory nerve and cochlear nucleus magnocellularis of the barn owl, *Tyto alba*. *J. Neurosci.*, **17**, 3312–3321.
- Kurian, R., Krupp, N.L. & Saunders, J.C. (2003) Tip link loss and recovery on chick short hair cells following intense exposure to sound. *Hear. Res.*, **181**, 40–50.
- Lifshitz, J., Furman, A.C., Altman, K.W. & Saunders, J.C. (2004) Spatial tuning curves along the chick basilar papilla in normal and sound-exposed ears. *J. Assoc. Res. Otolaryngol.*, **5**, 171–184.
- Manley, G.A. & Köpl, C. (1998) Phylogenetic development of the cochlea and its innervation. *Curr. Opin. Neurobiol.*, **8**, 468–474.
- Manley, G.A., Kaiser, A., Brix, J. & Gleich, O. (1991) Activity patterns of primary auditory-nerve fibres in chickens: development of fundamental properties. *Hear. Res.*, **57**, 1–15.
- Manley, G.A., Köpl, C. & Yates, G.K. (1997) Activity of primary auditory neurons in the cochlear ganglion of the emu *Dromaius novaehollandiae*: spontaneous discharge, frequency tuning, and phase locking. *J. Acoust. Soc. Am.*, **101**, 1560–1573.
- Mardia, K.V. (1972) *Statistics of Directional Data*. Academic Press, London.
- Marsh, R.R., Xu, L.R., Moy, J.P. & Saunders, J.C. (1990) Recovery of the basilar papilla following intense sound exposure in the chick. *Hear. Res.*, **46**, 229–237.
- Martin, P. & Hudspeth, A.J. (1999) Active hair-bundle movements can amplify a hair cell's response to oscillatory mechanical stimuli. *Proc. Natl Acad. Sci. U.S.A.*, **96**, 14 306–14 311.
- McFadden, E.A. & Saunders, J.C. (1989) Recovery of auditory function following intense sound exposure in the neonatal chick. *Hear. Res.*, **41**, 205–215.
- Moser, T. & Beutner, D. (2000) Kinetics of exocytosis and endocytosis at the cochlear inner hair cell afferent synapse of the mouse. *Proc. Natl Acad. Sci. U.S.A.*, **97**, 883–888.
- Narins, P.M. & Wagner, I. (1989) Noise susceptibility and immunity of phase locking in amphibian auditory-nerve fibers. *J. Acoust. Soc. Am.*, **85**, 1255–1265.
- Palmer, A.R. & Russell, I.J. (1986) Phase-locking in the cochlear nerve of the guinea-pig and its relation to the receptor potential of inner hair-cells. *Hear. Res.*, **24**, 1–15.
- Paolini, A.G., FitzGerald, J.V., Burkitt, A.N. & Clark, G.M. (2001) Temporal processing from the auditory nerve to the medial nucleus of the trapezoid body in the rat. *Hear. Res.*, **159**, 101–116.
- Papoulis, A. (1984) *Probability, Random Variables, and Stochastic Processes*. McGraw-Hill, New York.
- Parsons, T.D., Lenzi, D., Almers, W. & Roberts, W.M. (1994) Calcium-triggered exocytosis and endocytosis in an isolated presynaptic cell: capacitance measurements in saccular hair cells. *Neuron*, **13**, 875–883.
- Plontke, S.K., Lifshitz, J. & Saunders, J.C. (1999) Distribution of rate-intensity function types in chick cochlear nerve after exposure to intense sound. *Brain Res.*, **842**, 262–274.
- Poje, C.P., Sewell, D.A. & Saunders, J.C. (1995) The effects of exposure to intense sound on the DC endocochlear potential in the chick. *Hear. Res.*, **82**, 197–204.
- Pugliano, F.A., Wilcox, T.O., Rossiter, J. & Saunders, J.C. (1993) Recovery of auditory structure and function in neonatal chicks exposed to intense sound for 8 days. *Neurosci. Lett.*, **151**, 214–218.
- Ramakrishna, R., Kurian, R., Saunders, J.C. & Gratton, M.A. (2004) Recovery of the tegmentum vasculosum in the noise exposed chick. *Abst. Assoc. Res. Otolaryngol.*, **24**, 67.
- Sachs, M.B., Woolf, N.K. & Sinnott, J.M. (1980) Response properties of neurons in the avian auditory system: Comparisons with mammalian homologues and consideration of the neural coding of complex stimuli. In Popper, A.N. & Fay, R.R. (Eds), *Comparative Studies of Hearing in Vertebrates*. Springer-Verlag, New York, pp. 323–353.
- Salvi, R.J., Saunders, S.S., Powers, N.L. & Boettcher, F.A. (1992) Discharge patterns of cochlear ganglion neurons in the chicken. *J. Comp. Physiol. [A]*, **170**, 227–241.
- Salvi, R.J., Saunders, S.S., Hashino, E. & Chen, L. (1994) Discharge patterns of chicken cochlear ganglion neurons following kanamycin-induced hair cell loss and regeneration. *J. Comp. Physiol. [A]*, **174**, 351–369.
- Saunders, J.C. & Salvi, R.J. (2006) The recovery of function in the avian auditory system following ototrauma. In Salvi, R.J., Fay, R.R. & Popper, A.N. (Eds), *Regeneration and Repair in the Auditory System*. Springer-Verlag, New York.
- Saunders, J.C., Dear, S.P. & Schneider, M.E. (1985) The anatomical consequences of acoustic injury: a review and tutorial. *J. Acoust. Soc. Am.*, **78**, 833–860.
- Saunders, J.C., Adler, H.J. & Pugliano, F.A. (1992) The structural and functional aspects of hair cell regeneration in the chick as a result of exposure to intense sound. *Exp. Neurol.*, **115**, 13–17.
- Saunders, J.C., Doan, D.E., Cohen, Y.E., Adler, H.J. & Poje, C.P. (1996a) Recent observations on the recovery of structure and function in the sound-damaged chick ear. In Salvi, R.J. & Henderson, D. (Eds), *Auditory System Plasticity and Regeneration*. Thieme Medical Publishers, New York, pp. 62–83.
- Saunders, J.C., Doan, D.E., Poje, C.P. & Fisher, K.A. (1996b) Cochlear nerve activity after intense sound exposure in neonatal chicks. *J. Neurophysiol.*, **76**, 770–787.
- Saunders, J.C., Ventetuolo, C.E., Plontke, S.K. & Weiss, B.A. (2002) Coding of sound intensity in the chick cochlear nerve. *J. Neurophysiol.*, **88**, 2887–2898.
- Siegel, J.H. (1992) Spontaneous synaptic potentials from afferent terminals in the guinea pig cochlea. *Hear. Res.*, **59**, 85–92.
- Smolders, J.W., Ding-Pfennigdorff, D. & Klinke, R. (1995) A functional map of the pigeon basilar papilla: correlation of the properties of single auditory nerve fibres and their peripheral origin. *Hear. Res.*, **92**, 151–169.
- Spassova, M., Eisen, M.D., Saunders, J.C. & Parsons, T.D. (2001) Chick cochlear hair cell exocytosis mediated by dihydropyridine-sensitive calcium channels. *J. Physiol.*, **535**, 689–696.
- Spassova, M., Avissar, M., Furman, A.C., Crumling, M.A., Saunders, J.C. & Parsons, T.D. (2004) Evidence that rapid vesicle replenishment of the synaptic ribbon mediates recovery from short-term adaptation at the hair cell synapse. *J. Assoc. Res. Otolaryngol.*, **5**, 376–390.
- Szymko, Y.M., Nelson-Adesokan, P.M. & Saunders, J.C. (1995) Stiffness changes in chick hair bundles following in vitro overstimulation. *J. Comp. Physiol. [A]*, **176**, 727–735.
- Wever, E.G. (1949) *Theory of Hearing*. Wiley, New York.
- Zidanic, M. & Fuchs, P.A. (1995) Kinetic analysis of barium currents in chick cochlear hair cells. *Biophys. J.*, **68**, 1323–1336.